論文 한국정밀공학회지 제 12권 제4호 1995. 4
Journal of the Korean Society of Precision Engineering Vol. 12. No 4. April. 1995.

종동력을 받는 자유 Timoshenko보의 안정성 해석에 미치는 두개의 부가질량의 영향

류 봉 조*, 杉山 吉彦**

The Influence of Two Attatched Masses on the Stability Analysis of a Free-Free Timoshenko Beam under a Follower Force

Bong-Jo Ryu,* Yoshihiko Sugiyama**

ABSTRACT

본 논문은 복수 집중질량을 갖고 제어 종동력을 받는 자유 Timoshenko보의 동적안정성에 관한 것으로, 비행중의 미사일이나 로켓의 연료탱크, Payload등의 기계장치부를 복수의 집중질량으로 간주하여 이러한 항공우주구조물들이 추진력인 종동력을 받을때에 대한 계의 동적 안정성을 판별한다. 수학적 모델에 대한 운동방정식은 확장된 해밀톤 원리를 이용한 유한요소법에 의해 유도되며, 복수 부가질량의 위치 및 크기변화, 센서의 위치 및 게인(gain)의 변화에 따른 계의 안정성 지도(stability maps)를 보여준다. 또한 보의 전단변형이나 회전관성의 효과 뿐만아니라, 추진력의 방향이 제어되는 경우와 제어되지 않는 경우에 대한 최대추진력 값이 수치 시뮬레이션을 통해 예측된다.

Key words : Controlled Follower Force, Dynamic Stability, A Free-Free Timoshenko Beam, Extended Hamilton's Principle

1. INTRODUCTION

There has been a strong demand for the investigation into vibration and stability of a free-free beam subjected to an end thrust induced by a rocket motor. The end thrust is a typical nonconservative force. A lot of papers have been published on the stability problem of nonconservative systems. Beal[1] studied dynamic stability of a free-free Euler-Bernoulli beam subjected to a controlled follower force. Matsumoto and Mote[2] investigated the time-delay effect of a follower thrust on the stability of free-free beams under a controlled follower force. Park and Mote[3] studied the maximum controlled follower force of a free-free beam carrying a concentrated mass. Kounadis and Katsikadelis[4] conducted

* 대전산업대학교 기계설계공학과
** 일본 대판부립대학 항공우주공학과

for the coupling effects on the flutter load of two concentrated masses of cantilevers under a follower force, and Wu[5] presented the stability problems of a free-free beam under an axial thrust. In contrast to these theoretical works, Sugiyama and his collaborators[6] conducted experiments on the flutter instability of a cantilevered column subjected to a follower force. The force was produced by the direct installation of a real solid rocket motor. It is very interesting that they confirmed the good agreement between experiment and theoretical prediction. However, the effects of the rotary inertia and shear deformation of beams under a follower force have not been investigated so far in a due consideration. Until now, a few researchers[7-9] have studied the dynamic stability of Timoshenko beams. Particulaly the effect of the two concentrated masses on the stability of beams has not been investigated sufficiently so far. The first author and Park[10] has shown stability characteristics according to the variation of shear deformation and rotary inertia parameters.

2. THEORETICAL ANALYSIS AND METHOD OF CALCULATION

2.1 Mathematical Modeling

Slender rockets or missiles may have heavy machinery components, such as fuel tanks, pay loads and so on. These components can be assumed as concentrated masses. Fig. 1 shows a mathematical model of a free-free uniform Timoshenko beam containing two concentrated masses. It is assumed that the beam model is subjected to a constant follower force P. The beam has length L, bending stiffness EI, mass per unit length ρA. Two additional concentrated masses M_1 and M_2 with rotary inertias J_1 and J_2, respectively, are located on the centerline of the beam. It is assumed that one of

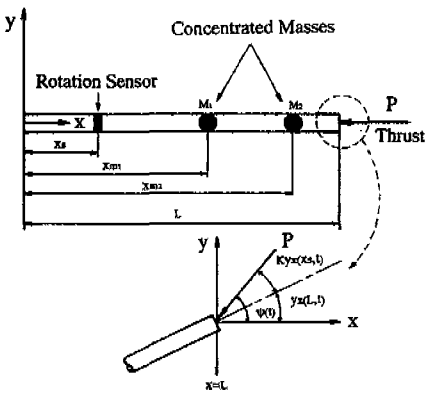

Fig. 1 A free-free Timoshenko beam carrying two concentrated masses

the two concentrated masses, M_2, is constant and fixed at a specified position x_{m2}, while the other M_1 is variable at different position x_{m1}.

2.2 Fundamental Equations

The axial force at arbitrary point of the beam, $P^*(x)$, as shown in Fig. 1, is given by

$$P^*(x) = \frac{\{\rho Ax + M_1 H(x - x_{m1}) + M_2 H(x - x_{m2})\}P}{\rho AL + M_1 + M_2} \quad (1)$$

where $H(x)$ is a heviside step function at $x = 0$

The angle of rotation between the follower force and undeformed x axis of the beam at $x = L$, $\Psi(t)$, is controlled by the following law.

$$\Psi(t) = KY_x(x_s, t) + Y_x(L, t) \quad (2)$$

where K and x_s are the gain of the sensor and the sensor location, respectively. Subscripts for transverse displacement Y denote differentiation with respect to the subscripted variable.

The extended Hamilton's principle for the beam model is

$$\delta \int_{t_1}^{t_2} \underset{\pounds}{} dt + \int_{t_1}^{t_2} \delta W^N dt = 0 \quad (3)$$

where the Lagrangian £ is given by

$$\pounds = T - V + W_c \tag{4}$$

In Equations (3) and (4), the kinetic energy T, the strain energy V, the conservative work done W_c and the nonconservative virtual work done δW^N for the considered problem are given by

$$T = \frac{1}{2}\int_O^L (\rho A Y_t^2 + \rho I \phi_t^2)dx + \frac{1}{2}M_1 Y_t^2(x_{m1}, t) + \frac{1}{2}M_2 Y_t^2(x_{m2}, t) + \frac{1}{2}J_1\phi_t^2(x_{m1}, t) + \frac{1}{2}J_2\phi_t^2(x_{m2}, t) \tag{5}$$

$$V = \frac{1}{2}\int_O^L \{(EI\phi_x^2) + K_s AG(Y_x - \phi)^2\}dx \tag{6}$$

$$W_c = \frac{1}{2}\int_O^L P^*(x) Y_x^2 dx \tag{7}$$

$$\delta W^N = -P\Psi(t)\cdot\delta Y(L, t) \tag{8}$$

where k_s is the shear coefficient and G is the shear modulus.

Substitution of Equations (5)-(8) into Equation (3) leads to

$$\delta\int_{t_1}^{t_2}\{\frac{1}{2}\int_O^L (\rho A Y_t^2 + \rho I\phi_t^2)dx + \frac{1}{2}M_1 Y_t^2(x_{m1}, t) + \frac{1}{2}M_2 Y_t^2(x_{m2}, t) + \frac{1}{2}J_1\phi_t^2(x_{m1}, t) + \frac{1}{2}J_2\phi_t^2(x_{m2}, t) - \frac{1}{2}\int_O^L \{EI\phi_x^2 + K_s AG(Y_x - \phi)^2\}dx + \frac{1}{2}\int_O^L P^*(x)\cdot Y_x^2 dx\}dt - \int_{t_1}^{t_2} P\Psi(t)\cdot\delta Y(L, t)dt = 0 \tag{9}$$

where Y is the lateral displacement and ϕ the bending slope of the beam.

Now, the finite element method is employed to discretize the Equation (9) into a dynamical system having a finite degrees of freedom.

For simplicity, it is convenient to introduce the local coordinates and their dimensionless quantities.

$$x' = x - (i-1)l, \quad x'_{m1} = (a_1 - 1)l, \quad x'_{m2} = x_{m2} - (a_2 - 1)l, \quad x'_s = x_s - (b-1)l \tag{10}$$

$$\xi = x'/l, \quad \xi_{m1} = x'_{m1}/l, \quad \xi_{m2} = x'_{m2}/l, \quad \xi_s = x'_s/l, \quad \eta = Y/l \tag{11}$$

where i indicates the ith element of the beam model, a_1 and a_2 denote the elements of two attatched concentrated masses, repectively, b depicts the element which the sensor is attatched.

With the quantities defined in Equations (10)-(11), and for N finite elements of equal length, the weak form of the field Equation (9) can be written by

$$\sum_{i=1}^{N}\int_0^1 \{\rho A l^3 \eta_{tt}(\xi,t)^{(i)}\delta\eta(\xi,t)^{(i)} + \rho I l\phi_{tt}(\xi,t)^{(i)}\delta\phi(\xi,t)^{(i)} + \frac{EI}{l}\phi_\xi(\xi,t)^{(i)}\delta\phi_\xi(\xi,t)^{(i)} + K_s AGl(\eta_\xi(\xi,t)^{(i)} - \phi(\xi,t)^{(i)})\delta(\eta_\xi(\xi,t) - \phi(\xi,t)^{(i)}) - \frac{\rho A(i-1+\xi)l^2}{\rho AL + M_1 + M_2} P\eta_\xi(\xi,t)^{(i)}\delta\eta_\xi(\xi,t)^{(i)} - \int_0^1 \frac{M_1 lH(\xi - \xi_{m1})}{\rho AL + M_1 + M_2} P\eta_\xi(\xi,t)^{(a_1)}\delta\eta_\xi(\xi,t)^{(a_1)}d\xi - \sum_{i=a_1+1}^{a_2}\int_0^1 \frac{M_1 lP\eta_\xi(\xi,t)^{(i)}\delta\eta_\xi(\xi,t)^{(i)}d\xi}{\rho AL + M_1 + M_2} - \int_0^1 \frac{M_2 lH(\xi - \xi_{m1})}{\rho AL + M_1 + M_2} P\eta_\xi(\xi,t)^{(a_2)}\delta\eta_\xi(\xi,t)^{(a_2)}d\xi - \sum_{i=a_1+1}^{a_2}\int_0^1 \frac{M_1 lP\eta_\xi(\xi,t)^{(i)}\delta\eta_\xi(\xi,t)^{(i)}d\xi}{\rho AL + M_1 + M_2} + M_1 l^2\eta_{tt}(\xi_{m1},t)^{(a_1)}\delta\eta(\xi_{m1},t)^{(a_1)} + J_1\phi_{tt}(\xi_{m1},t)^{(a_1)}\delta\phi(\xi_{m1},t)^{(a_1)} + M_2 l^2\eta_{tt}(\xi_{m1},t)^{(a_2)}\delta\eta(\xi_{m1},t)^{(a_2)} + J_2\phi_{tt}(\xi_{m2},t)^{(a_2)}\delta\phi(\xi_{m2},t)^{(a_2)} + Pl\{K\eta_\xi(\xi_s,t)^{(b)} + \eta_\xi(1,t)^{(N)}\}\delta\eta(1,t)^{(N)} = 0 \tag{12}$$

For convenience, the following non-dimensional parameters are introduced:

$$\lambda^2 = \frac{\rho AL^4 s^2}{EI}, \quad R = \frac{I}{AL^2}, \quad S = \frac{K_s AGL^2}{EI}, \quad Q = \frac{PL^2}{EI} \tag{13}$$

$$\alpha_1 = \frac{M_1}{\rho AL}, \quad \beta_1 = \frac{J_1}{\rho AL^3}, \quad \alpha_2 = \frac{M_2}{\rho AL}, \quad \beta_2 = \frac{J_2}{\rho AL^3} \tag{14}$$

$$\mu_1 = \frac{x_{m1}}{L}, \quad \mu_2 = \frac{x_{m2}}{L}, \quad \nu = \frac{x_s}{L} \tag{15}$$

In Equations (13)-(15), S is the shear deformation parameter, R the rotary inertia parameter, ν the sensor location, μ_1 and μ_2 are the

locations of two concentrated masses, respectively.

The solution to Equation(12) can be put into the forms:

$$\eta(\xi,t) = \eta(\xi)e^{st}, \quad \phi(\xi,t) = \phi(\xi)e^{st} \tag{16}$$

The coordinates functions $\eta(\xi)$ and $\phi(\xi)$ can be written in the forms:

$$\eta(\xi)^{(i)} = a^T(\xi)H^{(i)}, \quad \phi(\xi)^{(i)} = a^T(\xi)\Phi^{(i)} \tag{17}$$

where $H^{(i)}$ and $\Phi^{(i)}$ are generalized coordinate vectors, $a^T(\xi)$ is the shape function vector, and superscript T denotes the transpose of the matrix.

Substitution of Equations(16)-(17) into Equation(12) results in the matrix form.

$$\{\lambda^2[M]^* + [K_I]^* + Q[K_{II}]^*\}\{V\} = 0 \tag{18}$$

where {V} is as follows:

$$\{V\}^T = \{H^T \quad \Phi^T\} \tag{19}$$

The stabiliity of the Timoshenko beam model can be established by finding charateristic eigenvalues of Equation(18).

2.3 Stability Analysis

The stability of the considered system is determined by adopting the asymptotic criteria. The eigenvalue of the Equation(18) is related to the exponents s which is defined by the first of Equation(13). Thus, Equation(18) gives different characteristic values of the slightly disturbed system for every applied load.

If all characteristic roots, λ, are found, then the following stability criterion can be stated :

The system is stable, if the real parts of all the characteristic roots λ are negative value.

The system is unstable, if at least one of the characteristic roots λ has a positive real value.

The system is neutrally stable, if at least one of the characteristic roots λ has a zero real part and all others are negative.

3. NUMERICAL RESULTS AND DISCUSSION

Presented results were obtained by adopting 8 uniform finite element approximation of the free-free Timoshenko beam model. Corresponding eigensolutions can be obtained by solving numerically the matrix equation of motion. The effect of shear deformation and rotary inertia of the beam, and the position of the concentrated masses on the dynamic stability of the beam are investigated.

3.1 Stability without force direction control

If K = 0.0, the beam under a tangential follower force has two zero eigenvalues related to rigid body translation and rotation. However, since the zero eigenvalues do not involve bending of the beam, we consider the first two non-zero eigenvalues for beam bending to analyze stability.

The calculated stability maps are shown in Fig. 2. In these figure, S,D,F denote stable, divergence and flutter regions, respectively. The instability type depends upon the magnitude and location of the concentrated masses. When the location of concentrated mass, μ_1, has the value less than 0.5, the flutter force is reduced with increasing concentrated mass. Regardless of the location of concentrated mass, μ_2, the widest region of stability exists for the mass location of $\mu_1 = 0.7$. The critical follower force was calculated according to the variation of the locations of μ_1 and μ_2. In this figure, however, the second concetrated mass was fixed to the position of $\mu_1 = 0.1$.

Dependence of stability upon the magnitude of concentrated mass is shown in Fig. 3. It is seen that for $\alpha_1 = 0.0$, $\alpha_2 = 0.05$, $\beta_1 = 0.0$, $\beta_2 = 0.0$,

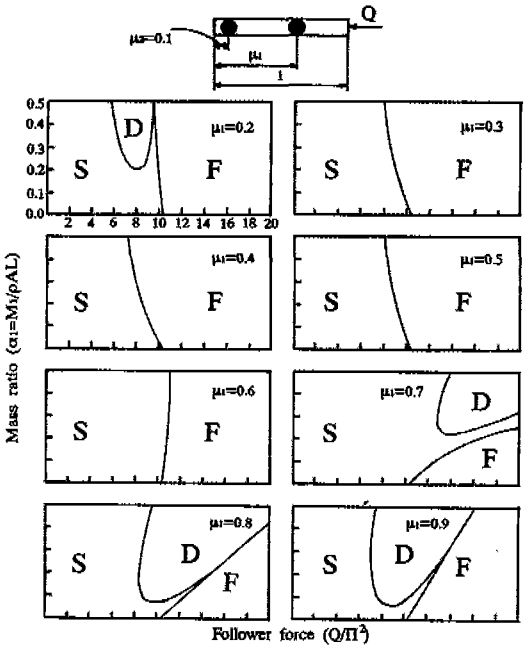

Fig. 2 Stability maps of a free-free Timoshenko beam without force direction control ($S = 10^3$, $R = 0.0$, $J_1 = J_2 = \beta_1 = \beta_2 = 0.0$, $\mu_2 = 0.1$, $\alpha_2 = 0.05$)

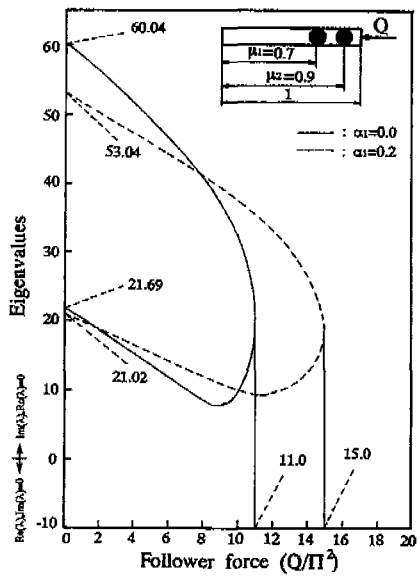

Fig. 3 Critical follower force depending upon the magnitude of concentrated mass ($S = 10^3$, $R = 0.0$, $J_1 = J_2 = \beta_1 = \beta_2 = 0.0$, $\alpha_2 = 0.05$, $K = 0.0$)

flutter type instability takes place for $Q_{cr}/\pi^2 \geq 11.0$, while the flutter force when $\alpha_1 = 0.2$, $\alpha_2 = 0.05$, $\beta_1 = 0.0$, $\beta_2 = 0.0$, satisfies $Q_{cr}/\pi^2 \geq 15.0$. Therefore Fig. 3 leads to the important conclusion that additional effect of concentrated mass results in the increase of critical follower force.

Fig. 4 shows the relationship between the follower force and rotary inertia parameter of the beam. The flutter force for rotary inertia parameter $R = 0.01$ decreases by about 23.1 percent comparing that for $R = 0.0$. For the small $R \leq 0.001$, however, the variation of rotary inertia of the beam affects only slightly the critical follower force.

3.2 Stability with force direction control

It is assumed now that the follower force is controlled by the proportional feedback of the rotation of the beam at $x = x_s$. If $K > 0$, only a zero eigenvalue associated with rigid body translation exists. Thus, it is justified again to consider the first two nonvanishing eigen-

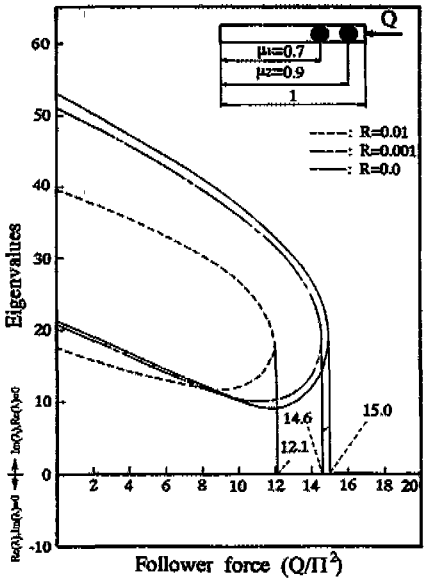

Fig. 4 Critical follower force depending upon rotary inertia of the beam in case of no direction control ($S = 10^3$, $J_1 = J_2 = \beta_1 = \beta_2 = 0.0$, $\alpha_1 = 0.2$, $\alpha_2 = 0.05$)

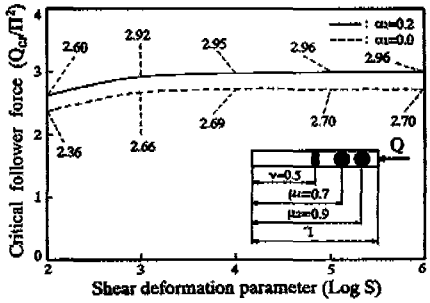

Fig. 5 Variation of critical follower force with shear deformation of beam in the case of direction control (R = 0.0, $J_1=J_2=\beta_1=\beta_2=0.0$, $\alpha_2=0.05$, K = 1.0)

values for beam bending.

The effect of shear deformation parameter S on the critical follower force is demonstrated in Fig. 5. Comparing the results for $S=10^2$ and $S=10^3$, increasing shear deformation parameter results in 13.8 percent increase in the critical follower force. For $S\geq10^4$, shear deformation parameter S has negligible effect on the critical follower force. Also by comparing $\alpha_1=0.0$ with $\alpha_2=0.2$, it is found that an additional concentrated mass results in increase of the flutter force as the parameter S varies from 10^2 to 10^6.

Fig. 6 to 8 depict the type of instability (i.e. either divergence or flutter) at sufficiently large follower force depending on the sensor location and a concentrated mass. Regardless of the sensor location, divergence always

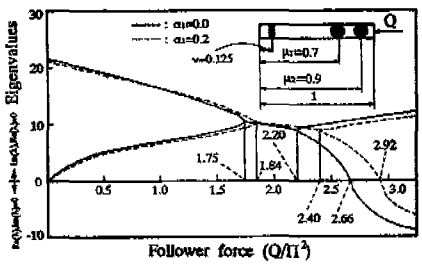

Fig. 6 Fundamental instability type of the beam with respect to the sensor location (S = 10^3, R = 0.0, $J_1=J_2=\beta_1=\beta_2=0.0$, $\alpha_2=0.05$, K = 1.0, $\nu=0.125$)

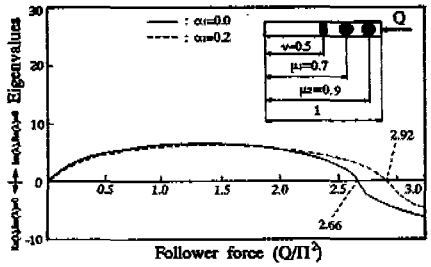

Fig. 7 Fundamental instability type of the beam with respect to the sensor location (S = 10^3, R = 0.0, $J_1=J_2=\beta_1=\beta_2=0.0$, $\alpha_2=0.05$, K = 1.0, $\nu=0.5$)

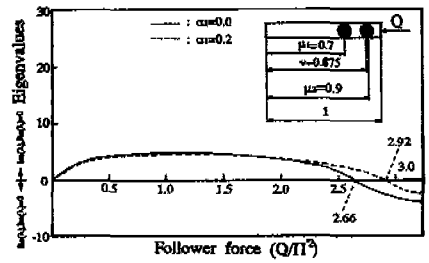

Fig. 8 Fundamental instability type of the beam with respect to the sensor location (S = 10^3, R = 0.0, $J_1=J_2=\beta_1=\beta_2=0.0$, $\alpha_2=0.05$, K = 1.0, $\nu=0.875$)

occurs at forces of $Q_{cr}/\pi^2=2.66$ when $\alpha_1=0.0$. Therefore, the sensor locations determine the instability types first encountered with increasing follower force. In this paper, the instability first encountered with a specified follower force is referred to as fundamental instability. For $\nu=0.125$, the fundamental instability is flutter when $1.75\leq Q_{cr}/\pi^2\leq2.20$. The critical follower force is dependent upon the magnitude of concentrated mass. The dashed lines show the critical follower force when the concentrated mass is added.

4. CONCLUDING REMARKS

The following conclusions were drawn through the present investigations.

4.1 Stability without force direction control

(1) The widest region of stability can be realized when the location of the concentrated mass, μ_1, has the value of 0.7.

(2) Small rotary inertia parameter $R \leq 0.001$, is ineffective in increasing the critical follower force.

4.2 Stability with force direction control

(1) Shear deformation parameter S negligibly affects on the critical force for $S \geq 10^4$.

(2) Type of fundamental instability depends on the sensor location.

(3) The flutter force is increased by adding a concentrated mass.

REFERENCES

1. Beal, T.R., "Dynamic Stability of a Flexible Missile under Constant and Pulsating Thrusts", AIAA Journal, Vol.3, pp.486-495, 1965.
2. Matsumoto, G.Y. and Mote JR, C.D., "Time Delay Instability in Large Order Systems with Controlled Follower Force", Journal of Dynamic Systems Measurement and Control" Vol.94, No.4, pp.330-334, 1972.
3. Park, Y.P. and Mote JR, C.D., "The Maximum Controlled Follower Force on a Free-Free Beam Carrying a Concentrated Mass", Journal of Sound and Vibration, Vol.98, No.2, pp.247-256, 1985.
4. Kounadis, A.N. and Katsikadelis, J.T., "Coupling Effects on a Cantilever Subjected to a Follower Force", Journal of Sound and Vibration, Vol.62, No.1, pp.131-139, 1979.
5. Wu, J.J., "On the Stability of a Free-Free Beam under Axial Thrust Subjected to a Directional Control", Journal of Sound and Vibration, Vol.43, pp.45-52, 1975.
6. Sugiyama, Y., Katayama, K. and Kinoi, S., "Experiment on Flutter of Canti-levered Columns Subjected to a Rocket Thrust", 31st AIAA/ASME/ASCE/AHS/ASC Structures, Structural Dynamics and Material Conference, pp.1893-1898, 1990.
7. Thomas, J. and Abbas, B.A.H., "Dynamic Stability of Timoshenko Beams by Finite Element Method", Journal of Engineering for Industry, Vol.98, pp.1145-1151, 1976.
8. Park, Y.P., "Dynamic Stability of a Free Timoshenko Beam under Controlled Follower Force", Journal of Sound and Vibration, Vol.113, pp.407-415, 1987.
9. Sato, K., "Vibration and Stability of a Clamped-Elastically Restrained Timoshenko Column under Nonconservative Load", JSME International Journal, Vol.34, No.4, pp.459-465, 1991.
10. Ryu, B.J. and Park, Y.P., "Effect of a Concentrated Mass on the Stability of a Free Timoshenko Beam under Controlled Follower Force", Proceedings of the KSME/JSME Vibration Conference'87, pp.309-318, 1987.